International Journal of Fatigue 32 (2010) 1233–1242

Contents lists available at ScienceDirect

International Journal of Fatigue

journal homepage: www.elsevier.com/locate/ijfatigue

High cycle fatigue strength of permanent mold and rheocast aluminum 357 alloy

Myriam Brochu [a,*], Yves Verreman [a], Frank Ajersch [a], Dominique Bouchard [b]

[a] École Polytechnique de Montréal, C.P. 6079, Succ. Centre-Ville, Montréal, Qc, Canada H3C 3A7
[b] Centre des Technologies de l'Aluminium, 501, Boul. de l'Université Est, Saguenay, Qc, Canada G7H 8C3

ARTICLE INFO

Article history:
Received 1 December 2009
Received in revised form 6 January 2010
Accepted 11 January 2010
Available online 18 January 2010

Keywords:
Aluminum 357 alloy
Casting
Semi-solid molding
High cycle fatigue
Microstructure

ABSTRACT

The high cycle fatigue resistances of aluminum–silicium–magnesium 357 alloy prepared by semi-solid forming (SSM) and conventional permanent mold casting (PM) are compared under fully reversed loading. Results, reported in *S–N* diagrams, show that rheocasting improves the as-cast alloy mean fatigue strength, by 36% at 10^7 cycles. Part of this improvement is explained by the fact that more SSM specimens are defect free than PM specimens. Comparison of the *S–N* diagrams also reveals that precipitation hardening slightly increases the fatigue strengths of the PM and SSM alloys, and that eutectic modification has no effect on the fatigue performance of the SSM alloy. Observation of small cracks using replicas shows the existence of crack growth decelerations at grain boundaries. No similar decelerations are observed when the crack enters a new α-Al cell within a grain. According to these results, it is proposed that in the absence of defects, the fatigue strength of aluminum alloy 357 is a function of the grain size (D) rather than of the secondary dendrite arm spacing (SDAS) or the spherical diameter of the alpha phase globules (φ_{sph}). Thus, it is concluded that the fatigue strength improvement of the SSM alloy is also related to the smaller grain of the rheocast specimens.

1. Introduction

The fatigue behaviour of conventionally cast (liquid state casting) Al–7%Si–Mg alloys (356 and 357) has been studied by many authors. Most of the experimental work published consists of the generation of *S–N* graphs and the characterization of crack propagation behaviour. Results available in the open literature lead to the following conclusions. The fatigue strength, at 10^7 cycles, of Al–7%Si–Mg for a T6 temper specimen can vary between 60 MPa [1] and 120 MPa [2]. Casting defects have a significant influence on the alloy fatigue strength [3–7]. The defect content, size and nature is known to be influenced by the casting process and the casting conditions that consequently have an effect on the alloy fatigue strength [8–10]. For example, hot isostatic pressing significantly improves the cast alloy fatigue life because it closes or suppresses volumetric defects such as shrinkage cavities and gas pores [6]. Semi-solid molding has a similar effect on fatigue strength because the amount of solidification shrinkage and entrapped gases is reduced by the injection of partially solidified mixtures. The fatigue strength of SSM specimen in T6 temper can vary between 60 MPa for low solid fraction (25%) and 140 MPa for solid fraction of 60% and an α-Al globule size of 38 μm [11].

For conventionally cast specimens, shrinkage cavities have been most frequently observed at the crack initiation sites [4,5,8,12–14]. In contrast, in semi-solid molding, oxide films are often found at crack initiation sites [7]. Although it is generally accepted that the reduction of fatigue life is a function of the defect size, there is no consensus on the critical defect size that affects the cast aluminum alloy fatigue strength. A critical defect size in the range of 25 μm has been proposed by Wang et al. [6] and Buffière et al. [15]. In addition to the casting defects, the influence of intrinsic microstructural features, such as grain size, secondary dendrites arm spacing (SDAS) and eutectic silicon morphology, on the alloy fatigue strength is not clear. There is no obvious correlation between microstructure, static properties and fatigue properties [12]. For example, heat treatment modifies the eutectic silicon morphology and the alpha phase hardness and has a strong influence on the yield strength of Al–Si–Mg alloys but it was found to have a limited effect on the alloy fatigue strength [3,5,8]. It is thought that the influence of defects prevails over the influence of intrinsic microstructural features. Nevertheless, in defect free specimens, the microstructural constituents play a role in fatigue crack nucleation and long crack propagation. Crack nucleation has been observed at the surface of eutectic silicon particles [2,14,16,17], or at intermetallic particles [2] and at persistent slip bands (PSB) [6,16,18]. The morphology of the alpha phase and of the eutectic silicon particles was also found to influence the crack propagation threshold in a study carried out on PM and SSM cast specimens [19]. However, the correlation between fatigue strength and microstructure has not yet been clearly interpreted in terms of specific damage mechanisms for conventionally cast and rheocast aluminum alloy 357.

* Corresponding author.
E-mail address: myriam.brochu@polymtl.ca (M. Brochu).

0142-1123/$ - see front matter © 2010 Elsevier Ltd. All rights reserved.
doi:10.1016/j.ijfatigue.2010.01.001

This paper presents the results of high cycle fatigue tests performed on aluminum–silicon–magnesium alloy 357 produced by liquid casting and rheocasting. The objective of this work is to identify the microstructural characteristics that have the most significant effect on the alloy fatigue strength. The influence of the defect content, the shape of the eutectic silicon particles, the shape and hardness of the primary phase and the grain size are investigated. Comparative *S–N* curves are presented for six different microstructures. Based on these results, on the fractographic and replica observations, a relationship between the alloy microstructure and its fatigue strength is proposed.

2. Materials and experimental procedure

2.1. Materials

Specimens were prepared from aluminum 357 alloy cast by two different processes. One batch consisting of uniform thickness rectangular plates, 14 millimetres thick, was gravity cast in a permanent mold (PM). Two other samples of rectangular wedge plates, with variable thickness from 16 to 9 millimetres, were rheomolded in the semi-solid state using an industrial pressure die casting machine. Details of the feed stock preparation were presented in a previous publication [20]. For the first batch of SSM plates, the chemical composition of the melt was adjusted as close as possible to the chemical composition of the permanent mold specimens. For the second batch of SSM plates, 25 ppm of strontium was added to the melt to modify the morphology of the eutectic silicon particles. For all batches, approximately 700 kg of A356.2 ingots were first melted in an electric furnace. These ingots had been previously grain refined by an addition of about 0.1% Ti with a Ti/B master alloy in the ratio of 5:1. Once the ingots were melted, magnesium was then added to comply with the 357 alloy composition. In some cases an aluminum-strontium master alloy was also added. Contaminants were removed with a fluxing agent (Promag RI) and argon was also injected in the melt with a rotary impeller. The average chemical compositions of the three batches of plates are given in Table 1.

Some of the PM and SSM-Sr plates were heat treated to T6 temper according to the following procedure: (1) Solution heat treatment in air at 540 °C for 1 h. (2) Warm water quench at 65 °C. (3) Ageing at 155 °C for 8 h. Since solution heat treatment created blisters in many of the SSM-Sr T6 plates, a T5 heat treatment was chosen as an alternative to T6 for some SSM and SSM-Sr plates. The T5 heat treatment sequence consisted of: (1) Extraction from casting mold at 350 °C. (2) Warm water quench at 65 °C. (3) Ageing at 170 °C for 6 h. Six different types of plates were produced: PM-F, PM-T6, SSM-F, SSM-T5, SSM-Sr-T5 and SSM-Sr-T6. All the plates were X-rayed and only the specimens with a quality corresponding to ASTM B108–03 grade B or better (discontinuities smaller than 1 millimetre) were used in this study.

2.2. Microstructural characterization

The microstructure of each type of plate was characterized by metallographic examination of polished and etched sections.

Table 1
Average chemical compositions (wt.%) analysed by optical spectroscopy using ASTM method E 1251(04).

Plates	Weight%								
	Si	Mg	Fe	Ti	Cu	Mn	Zn	Sr[a]	Al
PM	7.80	0.55	0.10	0.09	<0.01	<0.01	<0.01	<0.002	Bal.
SSM	8.10	0.62	0.07	0.12	<0.01	<0.01	<0.01	<0.002	Bal.
SSM-Sr	7.32	0.60	0.07	0.12	<0.01	0.01	<0.01	0.0025	Bal.

[a] Analysed by atomic absorption.

Table 2
Microstructural characteristics of the studied plates.

Plates	Temper[a]	D (μm) [range]	f_α (%) [range]	SDAS (μm) [range]	φ_{sph} (μm) [range]	L_{Si} (μm) [range]
PM	F	[400–1500]	[66–77]	[25–65]	–	[1–40]
PM	T6	[400–1500]	[66–77]	[22–62]	–	[1–40]
SSM	F	[50–350]	[62–75]	–	[5–185]	[1–42]
SSM	T5	[50–350]	[62–75]	–	[8–200]	[1–38]
SSM-Sr	T5	[40–400]	[61–73]	–	[3–230]	[0.5–10]
SSM-Sr	T6	[40–400]	[61–71]	–	[5–200]	[1–15]

[a] F: as-cast, T6: solution heat treated, quenched and peak aged, T5: quenched from the mold and peak aged.

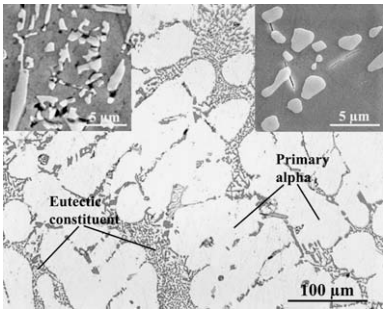

Fig. 1. General view of the microstructure of a PM-F plate. Upper left and right inserts are magnifications of the eutectic constituent of a PM-F and PM-T6 plate respectively.

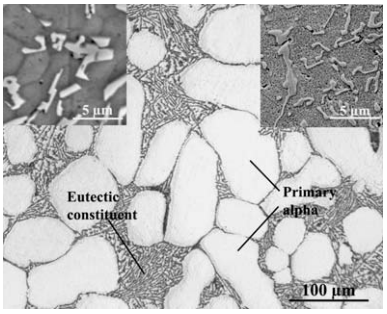

Fig. 2. General view of the microstructure of a SSM-F plate. Upper left and right inserts are magnifications of the eutectic constituent of a SSM-F and SSM-T5 plate respectively.

Transverse and longitudinal specimens showed an equiaxed and homogeneous microstructure for all types of plates. Measurements of microstructural features were carried out using a Nikon optical microscope and Clemex image analysis software. The following characteristics were measured: the grain size (D), the surface fraction of the primary alpha phase (f_α), the secondary dendrite arm spacing (SDAS) for the PM plates, the globule equivalent spherical diameter (φ_{sph}) for the SSM and SSM-Sr plates, and the maximum ferret size of the eutectic silicon particles (L_{Si}). The ranges of the measured microstructural characteristics are given in Table 2.

Typical microstructures of PM-F, SSM–F and SSM-Sr-T5 specimens are shown in Figs. 1–3 respectively. It can be observed that rheomolding produces a more globular alpha phase structure than liquid casting. Magnifications of the eutectic constituent are shown in the upper corners of each figure. PM-F, SSM-F and SSM-T5 plates have a comparable eutectic morphology composed of plate like silicon particles as shown in the left corner of Fig. 1 and the left and right corners of Fig. 2, respectively. The addition of strontium to the SSM-Sr melt resulted in a finer and more rounded eutectic sil-